

# Charge-transfer with graphene and nanotubes

Charge-transfer between electron–donor and –acceptor molecules is a widely studied subject of great chemical interest. Some of the charge-transfer compounds in solid state exhibit novel electronic properties. In the last two to three years, occurrence of molecular charge-transfer involving single-walled carbon nanotubes (SWNTs) and graphene has been demonstrated. This interaction gives rise to significant changes in the electronic properties of these nanocarbons. We examine charge-transfer phenomenon in graphene and SWNTs in this article in view of its potential utility in device applications.

C. N. R. Rao\* and Rakesh Voggu

International Centre for Materials Science, Chemistry and Physics of Materials Unit and CSIR Centre of Excellence in Chemistry Jawaharlal Nehru Centre for Advanced Scientific Research, Jakkur P. O., Bangalore 560064, India.

\*E-mail: [cnrrao@jncasr.ac.in](mailto:cnrrao@jncasr.ac.in)

Three types of nanocarbons have emerged in the last 25 years. These are fullerenes, carbon nanotubes and graphene. Fullerenes are zero-dimensional molecular compounds while carbon nanotubes are one-dimensional materials. Graphene is a two-dimensional network of carbon atoms with fascinating properties. All the three nanocarbons contain  $sp^2$  carbon atoms and one would expect certain similarities in the properties of these nanocarbons. One of the interesting characteristics that is worthy of comparison is molecular charge-transfer involving these nanocarbons.  $C_{60}$  is known to exhibit charge-transfer interaction with electron donating molecules such as organic amines both in the ground and excited states. What is more interesting is that both graphene and single-walled carbon nanotubes (SWNTs) interact with electron -donor and -acceptor molecules giving rise to significant changes in the electronic structure.

$C_{60}$  loves electrons and its salts exhibit fascinating magnetic and superconducting properties<sup>1</sup>. Recent investigations reveal that charge-transfer occurs between SWNTs and electron –donor and –acceptor molecules<sup>2,3</sup>, causing marked changes in the Raman and electronic spectra. Molecular charge-transfer is accompanied by the transformation of semiconducting nanotubes to metallic species and vice versa<sup>2,4</sup>. Graphene also undergoes charge-transfer interaction with electron -donor and -acceptor molecules<sup>5</sup>. Raman spectroscopy is eminently effective in probing charge-transfer interactions with graphene and SWNTs. In this article, we discuss molecular charge-transfer doping of graphene as well as of SWNTs and compare the effects with those found by chemical or electrochemical doping.

## Graphene

Graphene has become an exciting two-dimensional material with wondrous properties<sup>6–8</sup>. Some of the significant properties include

ballistic electron transport<sup>9</sup> and anomalous integer quantum Hall effect at room temperature<sup>10,11</sup>. Raman spectroscopy has emerged as an effective probe to characterize graphene samples in terms of the number of layers and their quality. Single-layer graphene shows the well-known G-band characteristic of the  $sp^2$  carbon network around  $1580\text{ cm}^{-1}$ . The D band around  $1350\text{ cm}^{-1}$  and D' band around  $1620\text{ cm}^{-1}$  are both defect-induced. The 2D band at  $\sim 2680\text{ cm}^{-1}$  differs in single and few-layer graphene and can be understood on the basis of the double resonance Raman process involving different electronic dispersions<sup>12</sup>. The 2D band can be employed to determine the number of layers in few-layer graphene. By combining Raman experiments with in-situ transport measurements of graphene in field-effect transistor geometry, it has been shown that the G-modes of single and bi-layer graphenes blue shift on doping with electrons as well as holes<sup>13,14</sup>. On the other hand, the 2D band blue-shifts on hole doping whereas it red shifts on doping with electrons. The relative intensity of the 2D band is quite sensitive to doping. Theoretical calculations based on time-dependent perturbation theory have been employed to explain the observed shifts of the G-band. Comparison between theory and experiment, however, is not entirely satisfactory at high doping levels ( $> 1 \times 10^{13}/\text{cm}^2$ ) and the disagreement is greater for the 2D band. In the case of bilayer graphene<sup>14</sup>, the blue-shift of the G-band with doping has contributions from phonon-induced inter-band and intra-band electronic transitions, thereby giving an experimental measure of the overlap integral between A and B atoms in the two layers. Furthermore, the in-plane vibration in bilayer graphene splits into a symmetric Raman active mode ( $E_g$ ) and an anti-symmetric infrared active mode ( $E_u$ ). Doping dependence of these modes has been examined by Raman scattering<sup>15</sup> and infrared reflectivity measurements<sup>16</sup>. The latter show a drastic enhancement of intensity and a softening of the mode as a function of doping, along with a Fano-like asymmetric line shape due to a strong coupling of the  $E_u$  mode to inter-band transitions.

There has been progress in the study of charge-transfer interactions of graphene with various electron donors and acceptors. The G-band softens progressively with the increasing concentration of electron-donor molecules such as aniline and tetrathiafulvalene (TTF) while the band stiffens with increasing concentration of electron-withdrawing molecules such as nitrobenzene and tetracyanoethylene (TCNE) as can be seen from Figs. 1 and 2<sup>5,17</sup>. Both electron-donors and -acceptors broaden the G-band. The full-width at half maximum (FWHM) of the G band increases on interaction with these molecules (Fig. 3a). The intensity of the 2D-band decreases markedly with the concentration of either donor or acceptor molecule. The ratio of intensities of the 2D and G bands,  $I(2D)/I(G)$ , is a sensitive probe to examine doping of graphene by electron-donor and -acceptor molecules (Fig. 3b). Dong *et al.*<sup>18</sup> have observed similar effects with single layer graphene on adsorption of various aromatic molecules while Brus *et al.*<sup>19</sup> have examined the effect of charge-transfer doping of graphene

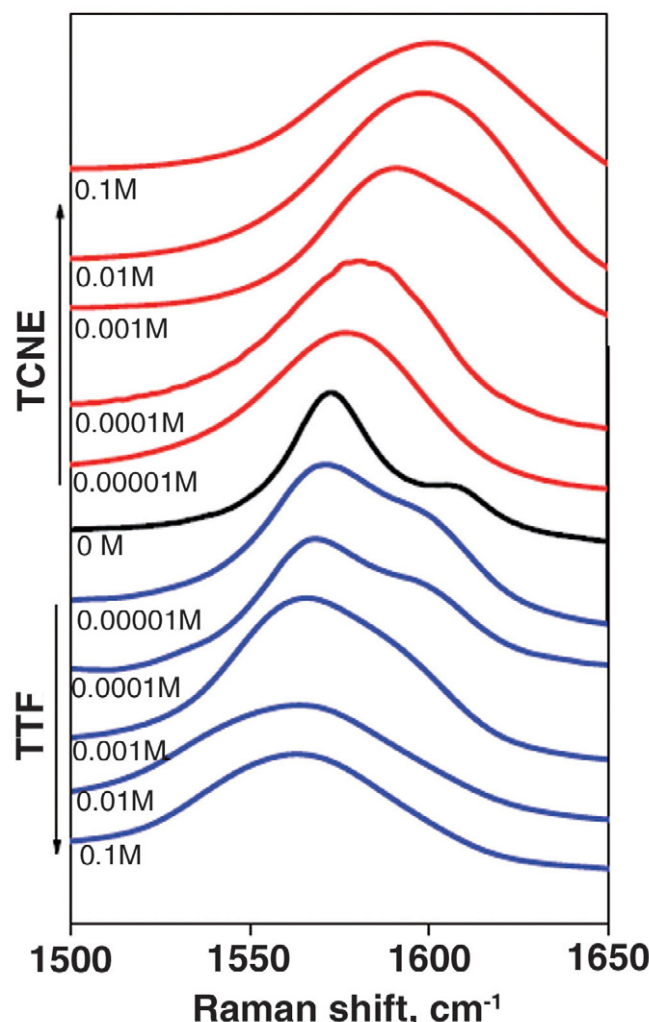


Fig. 1 Shifts of the Raman G-band of graphene caused by interaction with varying concentrations of TTF and TCNE<sup>17</sup>.

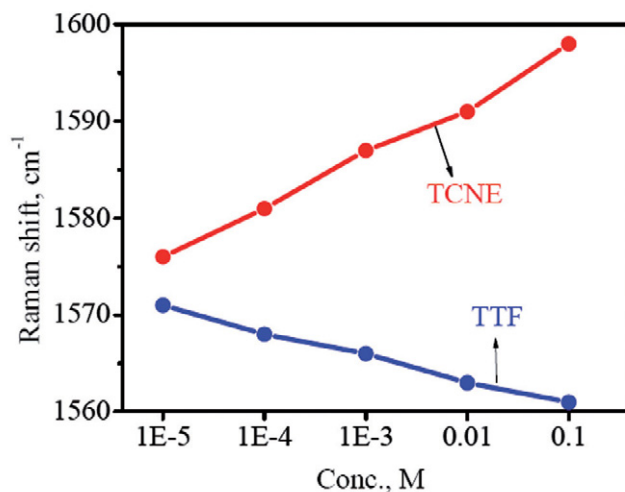


Fig. 2 Variation in the Raman G-band position of graphene on interaction with varying concentrations of electron-donor (TTF) and electron-acceptor (TCNE) molecules<sup>17</sup>.

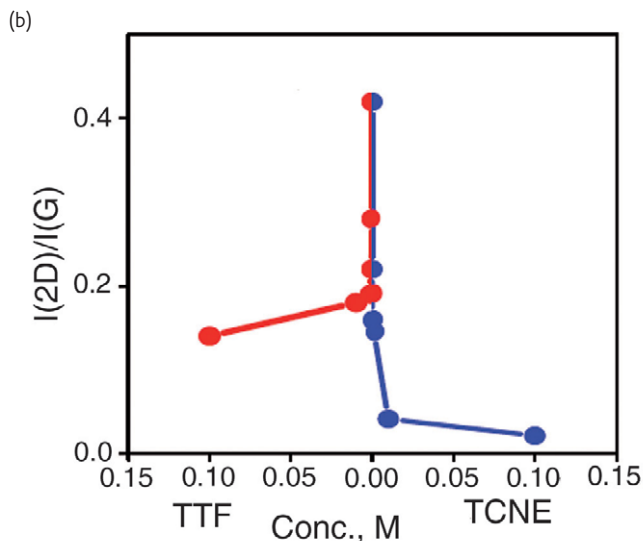
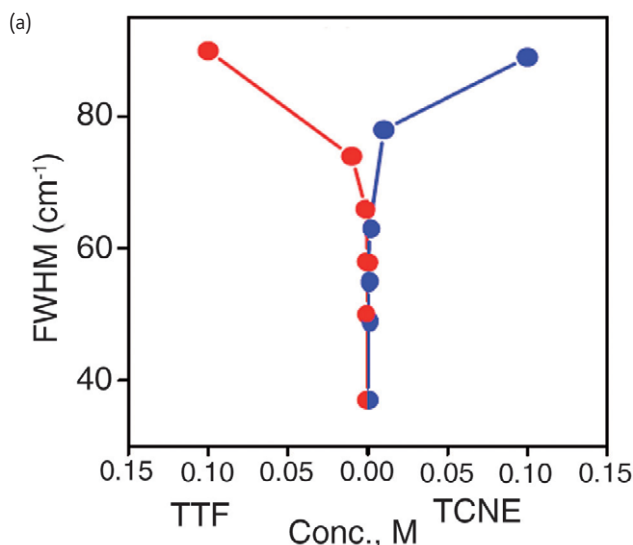


Fig. 3 Variation in the (a) FWHM and the (b) 2D/G intensity ratio with the concentration of TTF and TCNE<sup>17</sup>.

with bromine and iodine. They show that charge-transfer effects are greater on single and bi-layer graphenes compared to three and four-layer graphenes. Evidence for molecular charge-transfer involving graphene is also evidenced by the observation of charge-transfer bands in the electronic absorption spectra. Electrical resistivity of graphene varies in opposite directions on interaction with electron-donors and –acceptor molecules. The magnitude of interaction between graphene and donor/acceptor molecules seems to depend on the surface area of the graphene sample<sup>20</sup>. Isothermal titration calorimetry (ITC) measurements show that the interaction energies of graphene with electron-acceptor molecules are higher than those with -donor molecules<sup>21</sup>. DFT calculations confirm the occurrence of charge-transfer induced changes in graphene giving rise to mid-gap molecular levels with tuning of band gap region near the Dirac point

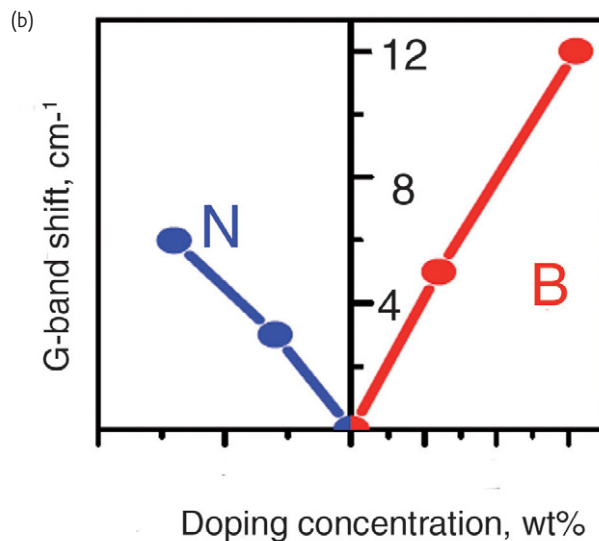
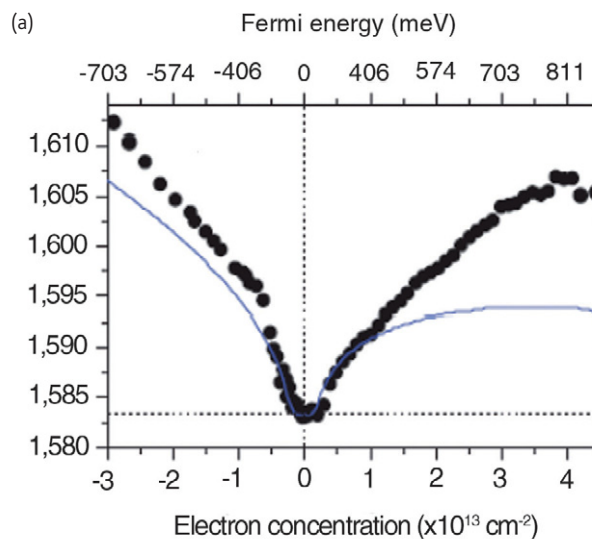
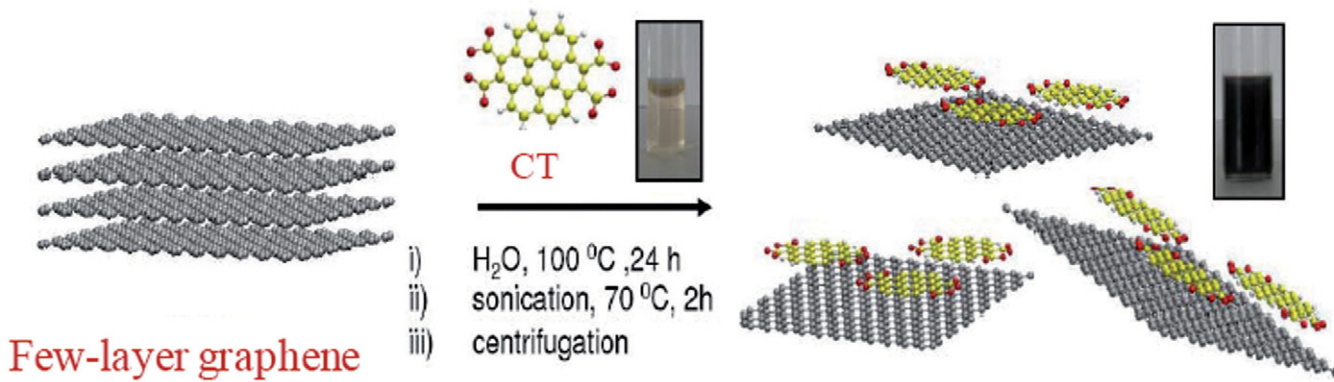


Fig. 4 (a) Position of the Raman G-band as a function of electron and hole doping<sup>13</sup>. (b) Shifts of the G-band caused by nitrogen and boron doping<sup>26</sup>.

and show how they are different from the effects of electrochemical doping<sup>22,23</sup>. It has been shown that n-type and p-type graphenes result from charge-transfer interaction of graphene with donor and acceptor molecules respectively. It is also predicted that the extent doping depends on the coverage of organic molecules. Synchrotron-based high-resolution photoemission spectroscopy studies reveal that charge transfer from graphene to adsorbed F<sub>4</sub>-TCNQ is responsible for the p-type doping of graphene<sup>24</sup>. Recent studies of the core-level spectra of the dopant molecules (TTF and TCNE) provide direct evidence for charge transfer involving graphene<sup>25</sup>.

It is interesting to compare the effects of doping graphene by gating<sup>13</sup> or chemical doping by boron and nitrogen<sup>26</sup> with those caused by molecular charge-transfer<sup>17</sup>. The G-band is shifted to higher frequencies when an electron acceptor molecule is adsorbed



Few-layer graphene

Fig. 5 Schematic illustration of exfoliation of few-layer graphene with CT to yield monolayer graphene-CT composites<sup>27</sup>.

on graphene, while it is shifted to lower frequencies when an electron donor molecule is adsorbed. This is in contrast to the gate-induced or chemical doping where the G-band increases in frequency for both the electron and hole doping (Compare Fig. 2 and 4). The difference may partly be due to local distortions caused in molecular interaction and this aspect needs further study. It is also possible that some of the graphene samples may have accidentally got doped (p or n type) giving rise to such differences. It would be instructive to investigate the effects of TTF and TCNE on B- and N- doped graphenes.

Organic molecules containing aromatic  $\pi$  systems can be used to solubilize and modify the electronic structure of graphene. Charge-transfer with coronene tetracarboxylate (CT) has been exploited recently to solubilize graphene sheets<sup>27</sup>. It was shown that the CT molecules help to exfoliate few-layer graphene and selectively solubilize single- and double-layer graphenes (Fig. 5). Graphene quenches the fluorescence of aromatic molecules, probably due to the electron transfer, a feature of possible use in photovoltaics. Charge-transfer from fluorescent molecules to graphene has been utilized in visualization of graphene sheets by fluorescence microscopy<sup>28</sup> and in the use of graphene as a substrate for resonance Raman spectroscopy<sup>29</sup>. Molecular charge-transfer affects the magnetic properties of graphene<sup>30</sup>. Magnetization of graphene decreases on adsorption of TTF and TCNE, interaction with TTF having a greater effect than with TCNE. It is difficult to know the exact cause of such differences, but effects related to molecular planarity and area as well as mechanical compression would be relevant factor.

Charge-transfer effects would be expected to be observed with graphene nanoribbons (GNRs) as well. Graphene nanoribbons are quasi one-dimensional materials with novel electronic, magnetic, optical and conduction properties<sup>31</sup>. Two different edge geometries, namely zigzag and armchair are possible, due to the finite termination of graphene which control the electronic properties of graphene nanoribbons. The periodic zigzag graphene nanoribbons (ZGNRs) show interesting localized electronic states at the edges<sup>32-34</sup>. These edge states are ferromagnetically ordered but antiferromagnetically coupled to each

other. Theoretical investigations have shown that ZGNRs become half-metallic when an external transverse electric field is applied but very high critical electric fields are required to achieve half-metallicity, suggesting that the realization of half-metallicity is practically difficult<sup>35,36</sup>. Chemical modification of edges either by passivation with functional groups such as H, NH<sub>2</sub>, NO, and CH<sub>3</sub><sup>37</sup> or the replacement of edge carbon atoms with boron (B) or nitrogen (N) atoms is suggested as an alternative way to induce half-metallicity in ZGNRs<sup>38,39</sup>. Molecular charge-transfer doping by the adsorption of various electron-donors and -acceptor molecules might lead to interesting changes in the electronic, magnetic and other properties of GNRs.

### Single-walled carbon nanotubes

Carbon nanotubes are one-dimensional (1D) materials with different chiralities and diameters<sup>40-42</sup>. SWNTs are formed by rolling two-dimensional graphene sheets into cylinders along a (n, m) lattice vector (C<sub>h</sub>) in the graphene plane, where n and m are integers. We can obtain the diameter and chiral angle from the (n, m) values. Nanotubes with chiral numbers n=m are metallic, and quasi metallic if n-m is divisible by 3. The other nanotubes are semiconducting. As-prepared SWNTs generally contain a mixture of metallic and semiconducting species. In conventional synthetic processes employed for SWNTs, metallic nanotubes constitute 33%, the remaining being semiconducting nanotubes. Metallic and semiconducting SWNTs are readily characterized by Raman and electronic spectra<sup>40,41,43,44</sup>. The radial breathing mode (RBM) in the Raman spectrum of SWNTs is useful for determining the diameter and the (n, m) values of the nanotubes. Electronic properties of the nanotubes can be predicted by using the Kataura plots based on the RBM bands. The Raman band of SWNTs centered around 1580 cm<sup>-1</sup> (G-band) exhibits a feature around ~1540 cm<sup>-1</sup> which is characteristic of metallic SWNTs<sup>43</sup>. The G-band can be deconvoluted to get the relative proportions of metallic and semiconducting species. Absorption spectra of SWNTs in the visible and near IR regions contain characteristic bands due to the metallic and semiconducting species.

Ability to tune the electronic properties of SWNTs is important for many applications. A control of the carrier type and concentration has been achieved by electrochemical doping or chemical doping. Through electrochemical top-gating, it is possible to achieve a high level of doping<sup>45</sup>. The electronic structure and phonon frequencies of SWNTs are affected on doping with electrons or holes. Changing the electronic properties of SWNTs by chemical means has attracted considerable attention. Chemical approaches employ covalent or noncovalent functionalization. Covalent functionalization methods include direct addition of fluorine atoms, cycloaddition reactions, radical and nucleophilic additions to side walls of nanotubes<sup>41,46</sup>. Another method is to introduce carboxylic groups on the side walls of SWNTs by oxidation. The carboxylic acid groups can be further transformed to amide or ester linkages. Attachment of various molecules also enables modification of the electronic structure of SWNTs<sup>41,46</sup>. The main problem with covalent functionalization is that it causes a change in the hybridization of carbon from  $sp^2$  to  $sp^3$ , and hence in the electronic structure. Excessive covalent functionalization completely destroys the electronic structure of SWNTs.

Noncovalent functionalization offers non-invasive approaches to modify SWNTs properties. Noncovalent modification can be brought by adsorption of aromatic compounds, surfactants or polymers and also through  $\pi$ - $\pi$  stacking and hydrophobic interaction. Earlier studies of noncovalent modification focused on the solubilization and exfoliation of SWNT bundles. Another aspect which has come into light in recent years is to modify the electronic structure of SWNTs by interaction with electron-donor and -acceptor molecules. This involves the adsorption of the electron-donor or -acceptor molecules on the surface of SWNTs. The advantage of molecular doping over other means is that one has an electronic system with less charged impurities. Furthermore, this effect of doping is reversible.

Doping of electrons and holes into SWNTs through molecular charge-transfer is of special interest<sup>2</sup>. Interaction of electron withdrawing molecules such as nitrobenzene and TCNE stiffen the Raman of SWNTs G-band while donating molecules such as TTF soften the G-band (Fig. 6a). The feature due to the metallic species around  $1540\text{ cm}^{-1}$  in the Raman spectrum nearly disappears on interaction of SWNTs with electron acceptors where as interaction of electron donors with SWNTs increases the metallic feature. It appears that electron donor molecules interact selectively with semiconducting SWNTs where as electron acceptors molecules interact with metallic SWNTs giving rise to possible metal  $\leftrightarrow$  semiconductor transitions. The changes in the Raman spectra are accompanied by changes in the electrical resistivity. The I-V curves become more nonlinear as one goes from aniline to nitrobenzene (Fig. 6b). The slope of the I-V curve also increases going from nitrobenzene to aniline, probably due to the presence of a higher proportion of metallic nanotubes in the presence of aniline. The above experiments were performed on mixture of metallic and semiconducting nanotubes. The experiments with pure

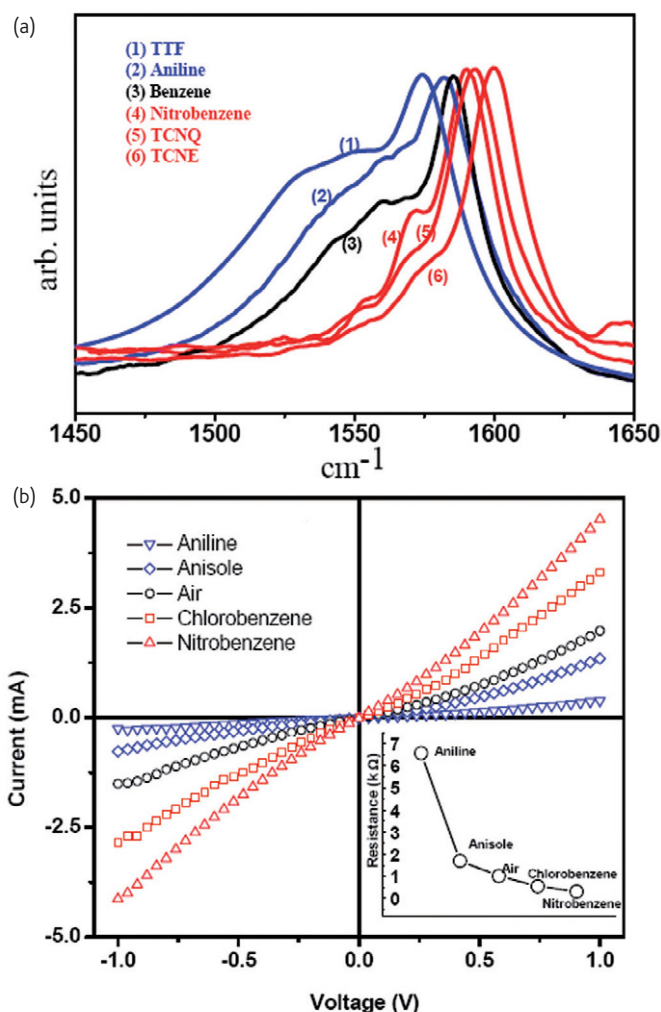


Fig. 6 (a) Effects of interaction of SWNTs with electron donor and acceptor molecules on G-band in the Raman spectra. (b) I-V characteristics of the SWNTs in air and in the presence of different benzene derivatives<sup>2</sup>.

metallic nanotubes separately show that on interaction with TCNE, the  $1540\text{ cm}^{-1}$  feature in Raman spectrum due to the metallic species disappears due to the change in the Fermi level of the nanotubes. TTF had no effect on the Raman spectrum of metallic SWNTs. Interaction of TTF with semiconducting carbon nanotubes, on the other hand, increases the intensity of the  $1540\text{ cm}^{-1}$  feature. This remarkable change in the electronic structure of SWNTs is entirely reversible. Electrochemical top gating of SWNTs leads to blue-shift in the G-band of SWNTs accompanied by a decrease in the line width with both electron and hole doping<sup>45</sup>.

ITC experiments on the interaction of SWNTs with molecules provide an insight into the affinities of the different molecules<sup>21</sup>. Interaction energies of electron acceptor molecules (e.g., TCNE) with SWNTs are higher than those of electron donor molecules (e.g., TTF). Metallic SWNTs interact reversibly with electron acceptor molecules such as TCNE, the interaction energy being higher than

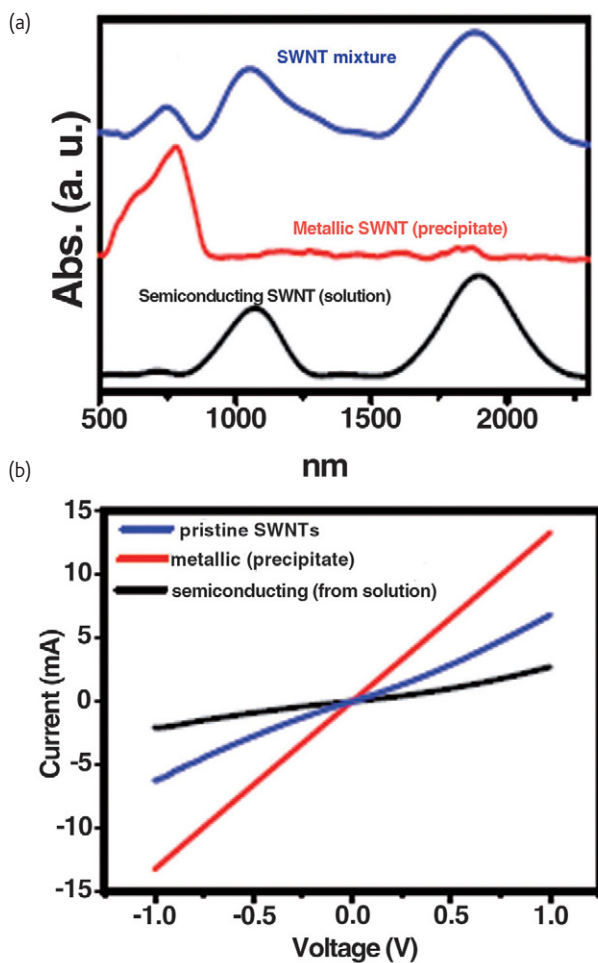


Fig. 7 (a) Optical absorption spectra and (b) I-V characteristics of pristine SWNTs (blue), precipitate (red) and SWNTs from solution (black)<sup>4</sup>.

with as-prepared SWNTs (containing a mixture of metallic and semiconducting species). The interaction energy of metallic nanotubes with a donor molecule such as TTF is negligible and could not be measured by ITC. ITC measurements clearly show that metallic nanotubes specifically interact with electron-withdrawing molecules. The interaction energy with acceptor molecules varies with the electron affinity as well as with the charge-transfer transition energy for different aromatics. Density functional theory calculations have shown that the nature of interaction is in physisorption regime and mainly governed by Coulombic forces<sup>47</sup>. The large band gap of semiconducting (8,0) SWNTs can be tuned through adsorption of selective organic molecules which gives mid gap localized molecular levels near the Fermi energy with tuning the band gap region. Metallic (5,5) SWNTs and semiconducting (8,0) SWNTs turn into semiconducting and metallic nanotubes respectively in the presence of adsorbed molecules.

Molecular charge-transfer between SWNTs and an appropriate  $\pi$ -system can be exploited for the effective separation of metallic and semiconducting nanotubes, since  $\pi-\pi$  interaction with aromatic molecules enables the solubilization of SWNTs<sup>4</sup>. Thus, the potassium

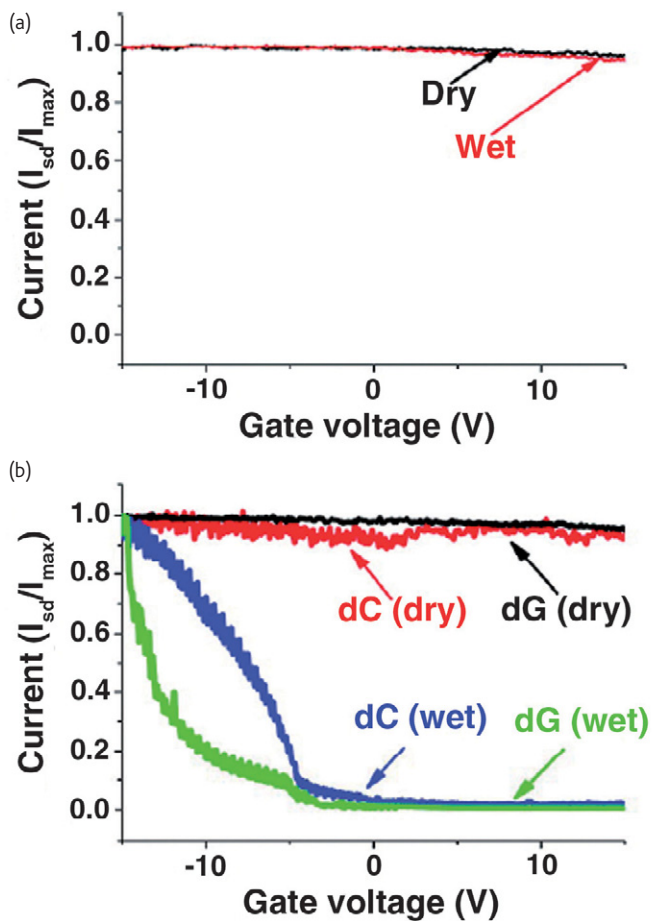


Fig. 8 Dependence of current of the ssDNA-SWNT hybrid on gate voltage. (a) A metallic behavior with SWNTs without DNA. (b) A p-type semiconductor behavior with the ssDNA-SWNT hybrid<sup>49</sup>.

salt of coronene tetracarboxylic acid (CS) which has a large  $\pi$  skeleton attached to four electron-withdrawing groups, exhibits charge-transfer interaction with SWNTs causing solubilization in aqueous medium. In this process, CS debundles the SWNTs and precipitates metallic SWNTs leaving semiconducting SWNTs in the solution. Fig. 7a shows the optical absorption spectra of SWNTs before and after separation. Pristine SWNTs show a nonlinear I-V curve while the metallic nanotubes show linear behavior with conductivities of 92.5 and 1538.5 mS/cm respectively at 300 K where as Semiconducting nanotubes exhibit a low conductivity of 53.5 mS/cm and a nonlinear I-V curve (Fig. 7b).

Nanoparticles of gold and platinum deposited on SWNTs also transform the semiconducting species to metallic ones due to Columbic charge-transfer<sup>48</sup>. Metal to semiconductor transition in SWNTs has been induced by helical wrapping of DNA<sup>49</sup>. Water appears to be critical to this reversible transition which accompanied by hybrid formation with DNA. It is predicted that a band gap can open up in metallic SWNTs wrapped with ssDNA in the presence of water molecules, due to charge-transfer (Fig. 8). Kim *et al.*<sup>50</sup> have shown that

**Instrument Citation**

- PerkinElmer instruments Lambda UV/VIS/NIR spectrometer.
- HORIBA JOBIN YVON LabRAM Raman spectrometer fitted with Raman mapping and heating and cooling stages.
- HORIBA JOBIN YVON Fluorolog spectrofluorometer fitted with single photon counting controller and iHR 320.

adsorption of  $\text{AuCl}_3$  to SWNTs results in high level of p-doping due to strong charge-transfer from the SWNTs to  $\text{AuCl}_3$  and they have shown that sheet resistance was systematically reduced with the increasing doping concentration. Ehli *et al.*<sup>51</sup> have shown that charge-transfer between SWNTs and perylene dyes leads to individualized nanotubes and they have observed radical ion-pair state is formed in the excited state. There are reports of charge-transfer interaction of SWNTs with  $\text{I}_2$  and  $\text{Br}_2$ <sup>52,53</sup>. Doping of double-walled carbon nanotubes with bromine and iodine has been investigated<sup>54,55</sup>. Charge-transfer doping of DWNTs has been used to distinguish between the behavior of the S/M and M/S outer/inner semiconducting (S) and metallic (M) tube configurations. The binding of electron-accepting molecules ( $\text{F}_4\text{TCNQ}$  and  $\text{NO}_2$ ) to SWNTs leads to a threshold voltage shift toward positive

gate voltages, while the binding of electron donating molecules ( $\text{NH}_3$  and PEI) leads to a shift toward negative gate voltages<sup>56–58</sup>. Field-effect transistor devices made of semiconducting SWNTs have been used to obtain quantitative information on charge-transfer with aromatic compounds<sup>59</sup>. Stoddart *et al.*<sup>60</sup> have fabricated SWNT/FET devices to investigate the electron/charge-transfer with the donor-acceptor SWNT hybrids. A SWNT/FET device, functionalized noncovalently with a zinc porphyrin derivative shows that SWNTs act as electron donors and that the porphyrin molecules act as the electron acceptors.

**Conclusions and outlook**

The discussion in the previous sections should make it clear how charge-transfer interaction of SWNTs with electron–donor and –acceptor molecules causes major changes in the Raman and electronic spectra of nanotubes. It is noteworthy that the transformation of semiconducting to metallic and vice versa is possible through charge-transfer interaction. Changes in the electronic and Raman spectra of graphene brought about by electron–donor and –acceptor molecules is equally fascinating. It should be possible to exploit the changes brought about by the molecular charge-transfer in these nanocarbons for device applications. mt

**REFERENCES**

1. Haddon, R. C., *Acc Chem Res* (1992) **25**, 127.
2. Voggu, R., *et al.*, *J Phys Chem C* (2008) **112**, 13053.
3. Shin, H.-J., *et al.*, *J Am Chem Soc* (2008) **130**, 2062.
4. Voggu, R., *et al.*, *J Am Chem Soc* (2010) **132**, 5560.
5. Das, B., *et al.*, *Chem Commun* (2008), 5155.
6. Geim, A. K., *Science* (2009) **324**, 1530.
7. Rao, C. N. R., *et al.*, *Angew Chem Int Ed* (2009) **48**, 7752.
8. Rao, C. N. R., *et al.*, *J Phys Chem Lett* (2010) **1**, 572.
9. Novoselov, K. S., *et al.*, *Science* (2004) **306**, 666.
10. Novoselov, K. S., *et al.*, *Nature* (2005) **438**, 197.
11. Zhang, Y., *et al.*, *Nature* (2005) **438**, 201.
12. Ferrari, A. C., *et al.*, *Phys Rev Lett* (2006) **97**, 187401.
13. Das, A., *et al.*, *Nat Nanotechnol* (2008) **3**, 210.
14. Das, A., *et al.*, *Phys Rev B* (2009) **79**, 155417.
15. Malard, L. M., *et al.*, *Phys Rev Lett* (2008) **101**, 257401.
16. Kuzmenko, A. B., *et al.*, *Phys Rev Lett* (2009) **103**, 116804.
17. Voggu, R., *et al.*, *J Phys Cond Mat* (2008) **20**, 472204.
18. Dong, X., *et al.*, *Small* (2009) **5**, 1422.
19. Jung, N., *et al.*, *Nano Lett* (2009) **9**, 4133.
20. Subrahmanyam, K. S., *et al.*, *Chem Phys Lett* (2009) **472**, 96.
21. Varghese, N., *et al.*, *J Phys Chem C* (2009) **113**, 16855.
22. Manna, A. K., and Pati, S. K., *Chem Asian J* (2009) **4**, 855.
23. Saha, S. K., *et al.*, *Phys Rev B* (2009) **80**, 155414.
24. Chen, W., *et al.*, *J Am Chem Soc* (2007) **129**, 10418.
25. Choudhury, D., *et al.*, *To be published*.
26. Panchakarla, L. S., *et al.*, *Adv Mat* (2009) **21**, 4726.
27. Ghosh, A., *et al.*, *Chem European J* (2010) **16**, 2700.
28. Kim, J., *et al.*, *J Am Chem Soc* (2009) **132**, 260.
29. Xie, L., *et al.*, *J Am Chem Soc* (2009) **131**, 9890.
30. Matte, H. S. S. R., *et al.*, *J Phys Chem C* (2009) **113**, 9982.
31. Dutta, S., and Pati, S. K., *J Mater Chem* (2010), doi: 10.1039/c0jm00261e.
32. Pisani, L., *et al.*, *Phys Rev B* (2007) **75** (6), 064418.
33. Rudberg, E., *et al.*, *Nano Lett* (2007) **7** (8), 2211.
34. Dutta, S., *et al.*, *Phys Rev B* (2008) **77** (7), 073412.
35. Son, Y.-W., *et al.*, *Nature* (2006) **444** (7117), 347.
36. Kan, E.-J., *et al.*, *App Phys Lett* (2007) **91** (24), 243116.
37. Li, Z., *et al.*, *J Am Chem Soc* (2008) **130** (13), 4224.
38. Dutta, S., *et al.*, *Phys Rev Lett* (2009) **102** (9), 096601.
39. Ci, L., *et al.*, *Nat Mater* **9** (5), 430.
40. Saito, R., *et al.*, *Physical Properties of Carbon Nanotubes*. Imperial College Press: London, 1998.
41. Rao, C. N. R., and Govindaraj, A., *Nanotubes and Nanowires: RSC Nanoscience & Nanotechnology series*. Royal Society of Chemistry: Cambridge, 2005.
42. Rao, C. N. R., *et al.*, *Nanoscale* (2009) **1**, 96.
43. Dresselhaus, M. S., *et al.*, *J Phys Chem C* (2007) **111**, 17887.
44. Strano, M. S., *J Am Chem Soc* (2003) **125**, 16148.
45. Das, A., *et al.*, *Phys Rev Lett* (2007) **99**, 136803.
46. Tasis, D., *et al.*, *Chem Rev* (2006) **106**, 1105.
47. Manna, A. K., and Pati, S. K., *Nanoscale* (2010) **2**, 1190.
48. Voggu, R., *et al.*, *J Phys Cond Mat* (2008) **20**, 215211.
49. Cha, M., *et al.*, *Nano Lett* (2009) **9**, 1345.
50. Kim, K. K., *et al.*, *J Am Chem Soc* (2008) **130**, 12757.
51. Ehli, C., *et al.*, *Nat Chem* (2009) **1**, 243.
52. Rao, A. M., *et al.*, *Nature* (1997) **388**, 257.
53. Chen, J., *et al.*, *Science* (1998) **282**, 95.
54. do Nascimento, G. M., *et al.*, *Nano Lett* (2008) **8**, 4168.
55. do Nascimento, G. M., *et al.*, *J Phys Chem C* (2009) **113**, 3934.
56. Shim, M., *et al.*, *J Am Chem Soc* (2001) **123**, 11512.
57. Kong, J., *et al.*, *Science* (2000) **287**, 622.
58. Takenobu, T., *et al.*, *Adv Mat* (2005) **17**, 2430.
59. Star, A., *et al.*, *Nano Lett* (2003) **3**, 1421.
60. Hecht, D. S., *et al.*, *Nano Lett* (2006) **6**, 2031.